Journal of Hydrology (2006) 327, 618–626

available at www.sciencedirect.com

SCIENCE DIRECT®

journal homepage: www.elsevier.com/locate/jhydrol

A physical model of particulate wash-off from rough impervious surfaces

Stephen B. Shaw *, M. Todd Walter, Tammo S. Steenhuis

Cornell University, Department of Biological and Environmental Engineering, Ithaca, NY 14853-5701, United States

Received 6 July 2005; received in revised form 20 January 2006; accepted 23 January 2006

KEYWORDS
Wash-off;
Impervious surface;
Nonpoint source pollution;
Urban hydrology

Summary Current urban water quality models rely on empirical, catchment-scale functions of particulate wash-off that do not clearly represent the governing physical erosion and transport processes. We proposed a saltation-type wash-off model in which particles are repeatedly ejected from an impervious surface by raindrop impacts and are transported laterally by overland flow while settling back to the surface. The rate that particles are ejected is proportional to rain intensity and the spatial density of particles on the surface. We found that for low particle spatial densities, ejection is proportional to spatial density, but for high spatial densities, the ejection rate is independent of spatial density. We tested our model against data from small (10.5×80 cm) flume experiments in which rain intensity and upslope overland flow could be independently controlled. We used a rough flume surface ($\sim$1 mm roughness element height) and sand particles (diameter = 500–590 μm). Rainfall rates, upslope overland flow rates, and initial particle amounts were varied among experiments with ranges of, 4.2–7.8 cm h^{-1}, 300–565 mL min^{-1}, and 0.01–0.07 g cm^{-2}, respectively. The model predictions agreed well with the experiments ($R^2 > 0.85$). This work provides a basis for developing new, uniquely mechanistic models for predicting ''wash-off'' from urban surfaces.

Introduction

Stormwater runoff from urban areas is recognized as a major source of water pollution. In addition to flushing dissolved materials from impervious surfaces, rainfall-runoff events also detach and transport substantial amounts of particulate matter (Sartor et al., 1974; Sansalone et al., 1998). Sartor and Boyd (1972) introduced the first particulate ''wash-off'' model, assuming the rate of particle loss on a catchment scale is directly related to the quantity of particulate available. Current urban stormwater models such as SWMM and HSPF are still based on this original lumped model (Tsihrintzis and Hamid, 1998; Bicknell et al., 1997). In addition to being spatially non-specific, models such as SWMM generally rely on extensive calibration of empirical wash-off coefficients (Tsihrintzis and Hamid, 1998), a fact that limits their

* Corresponding author. Tel.: +1 607 255 2463; fax: +1 607 255 4080.
E-mail address: sbs11@cornell.edu (S.B. Shaw).

0022-1694/$ - see front matter © 2006 Elsevier B.V. All rights reserved.
doi:10.1016/j.jhydrol.2006.01.024

predictive capabilities (Akan, 1988). Regulators' recent emphasis on reducing non-point source pollution has increased interest in implementing pollutant management practices in urban areas, a task requiring spatial specificity and predictive modeling. Greater insight into the underlying *physical mechanisms* of particulate detachment and transport will provide a more detailed understanding of the movement of pollutants in the urban landscape and ultimately more scientifically justifiable management practices for controlling urban storm runoff pollution.

There are few published explanations of physical wash-off mechanisms and these are generally borrowed from soil and stream channel erosion theory, albeit selectively and with limited rigorous, independent experimental validation. One early explanation asserted that the particle loss rate was related to bed shear stresses, although the concept was only supported indirectly, via calibration of a model to plot scale data (Akan, 1988). It is notable that this model neglected the role of rainfall-impact, assuming bed shear induced all particle movement and ignoring the broadly recognized concept of a threshold shear stress below which overland shear has no effect. With respect to soil erosion due to flows below the critical shear velocity, Moss et al. (1979) were perhaps the first to explicitly note the importance of so-called 'rain-flow transportation', a process in which raindrops on shallow water induce particle suspension in a manner similar to turbulence in deeper water. Deletic et al. (1997) proposed a wash-off model that recognized both threshold shear stress, as described by the Shield's curve (Graf, 1971), and rainfall effects. This model combined shear and rainfall effects on erosion as additive processes, different from the interactive roles of these processes described by Moss et al. (1979) and others (e.g., Kirkby, 1980; Rose, 1985; Rose et al., 1994). The Deletic et al. (1997) model achieved a reasonable fit to catchment-scale data with calibration coefficients, but no attempt was made to assess whether the spatial and temporal variations implicit in the model corresponded to physical reality.

Only limited work has been done to make direct observations. Vaze and Chiew (2003) attempted to directly isolate the respective roles of rainfall and runoff in particle entrainment and transport with plot experiments. Their deductions were only descriptive; they did not model the process. They concluded that rainfall- and runoff-forces were approximately equal and additive in inducing wash-off over a range of rainfall rates and flow depths.

This study proposes a simple mechanistic wash-off model and tests it with uncomplicated experiments to improve our understanding of the primary mechanisms behind wash-off on impervious surfaces — especially with respect to rain-impact — that research to-date has not clearly or consistently explained. This investigation's specific objectives are to: (1) develop a new, physically-based conceptual model to describe particle wash-off from rough, impervious surfaces for conditions in which 'rain-flow transportation' dominates and (2) test this conceptual model with controlled experiments that elucidate the underlying processes. The experiments, by necessity, employ flow conditions for which a critical overland shear stress is not attained in order to illustrate the interaction between overland flow and rainfall in rain-flow transport.

Theory

We consider wash-off of a thin layer of particles from a one-dimensional sloping plane. On this plane, particle movement occurs by a saltation-type process that can be conceptually described with a two-compartment model in which particles are either at rest on the rough surface or in motion suspended in the shallow flow (Fig. 1). Particles enter the shallow flow by raindrop-induced ejection at a rate e (g cm^{-2} min^{-1}) and settle-out of the shallow flow at a rate h (g cm^{-2} min^{-1}). While settling-out, suspended particles are advected in the overland flow at the same velocity as the overland flow. Particles on the rough surface layer undergo no movement unless hit by a raindrop.

Note that the 'rain-flow transport' modeled here is distinct from rain splash transport, in which a particle becomes airborne outside the shallow flow. In rain-flow transport the particle always remains within the flow layer. Airborne splash was not considered as the process is multidirectional, not unidirectional downslope, and net transport in any one direction is virtually zero (Moss et al., 1979).

Following Hairsine and Rose (1991) for the case in which flow does not exceed the threshold for particle entrainment, mass conservation of suspended particles in the water layer:

$$\frac{\partial M_s}{\partial t} + \frac{\partial v M_s}{\partial x} = e - h \tag{1}$$

where M_s is the suspended particle mass (g cm^{-2}), x is the downslope distance, and v is the fluid velocity (cm min^{-1}).

Particle mass on the surface, M_g (g cm^{-2}), at a distinct spatial position is given by:

$$\frac{dM_g}{dt} = h - e \tag{2}$$

Following Lisle et al.'s (1998) development of a stochastic particulate transport model initially derived to describe the movement of non-interacting particles:

$$e = aPM_g \tag{3}$$

where a (cm^{-1}) is an experimentally determined ''detachability'' constant that accounts for mass loss per drop and P is the precipitation rate (cm min^{-1}). This is similar to the expression proposed by Hairsine and Rose (1991) for soil erosion, although in their case e was gradually mitigated over the course of a storm by the development of a ''shield''

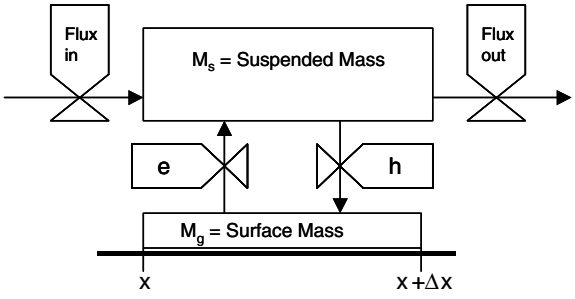

Figure 1 Flow diagram illustrating interaction between particles in suspension and particles on rough, impervious surface for a distinct control volume. Downslope particle motion occurs only when particles are in motion.

composed of large, heavy particles. In Eq. (3), the ejection rate is limited by particle availability on the surface, i.e., M_g. Based on experimental evidence presented later, we assume that there is some particle spatial density, M_0, above which the ejection rate will be independent of M_g, i.e, $e = aPM_0$. Note that, contrary to earlier consensus (e.g., Foster and Meyer, 1975; Liebenow et al., 1990; Laflen et al., 1991), recent research strongly suggests that the relationship between e and P is linear (Sharma et al., 1993, 1995; Jayawardena and Bhuiyan, 1999; Gao et al., 2003).

Particle settling rate is given by (Hairsine and Rose, 1991):

$$h = \frac{\alpha v_{set} M_s}{D} \quad (4)$$

where α adjusts bulk concentration to account for variations near the surface, v_{set} is the particle settling velocity, and D is the depth (cm). Since we are dealing only with very shallow flows and, thus, a minimal vertical concentration gradient in the water column, α is assumed to equal one.

Methods

Experimental set-up

Fig. 2 illustrates the central elements of our experimental apparatus. A unique attribute of our experimental set-up is that overland flow can be generated separately from rainfall. To distinguish between rainfall-generated runoff and overland flow applied directly at the upslope end of the flume, we will use the terms rainfall-runoff and upslope flow, respectively. An 80 cm long, 10.5 cm wide stainless steel flume was located beneath a computer-controlled rainmaker (Fig. 2). The flume had a 4% slope. A surface with a characteristic roughness length of approximately 1 mm was cut from a sheet of prismatic, polycarbonate diffuser used for recessed fluorescent light fixtures. The surface consisted of adjacent diamond-shaped indentions (Fig. 2). To ensure uniform flow, the surface was scoured with a wire brush to eliminate flow fingers and maintain uniform flow. A small Plexiglas stilling chamber with an overflow weir was used to control upslope flow. Flow into the stilling chamber was controlled with a variable speed peristaltic pump.

The rainmaker is the same as that used by Gao et al. (2003, 2004, 2005). Four hypodermic needles oscillated along two orthogonal tracks attached to the ceiling of the Soil and Water Lab at the Cornell University Department of Biological and Environmental Engineering, 3 m above the flume. Using the flour pellet method (Laws and Parsons, 1943), we found that the average drop radius at a rainfall rate of 0.07 cm min^{-1} was 0.092 cm and 0.082 cm at a rainfall rate of 0.13 cm min^{-1}. This measurement was in agreement with the observation that an increase in rainfall rate enhanced collisions between separate streams of flow from needles on the rain machine, leading to greater dispersion of droplets and consequently smaller droplets. Peristaltic

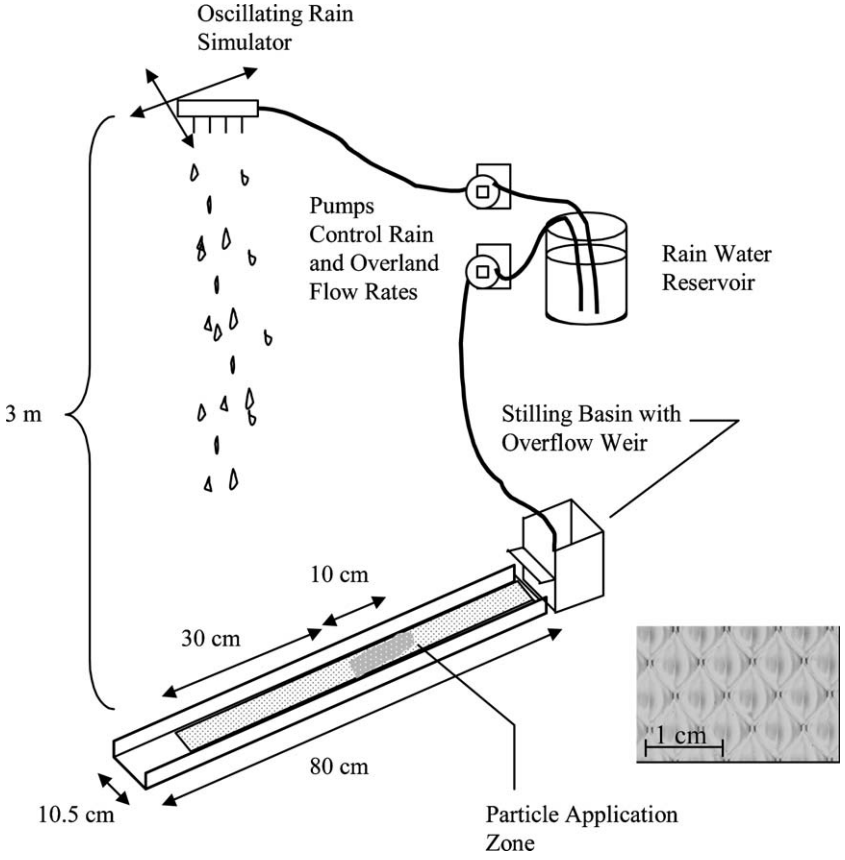

Figure 2 Schematic of experimental set-up and apparatus. Overland flow can be generated independently of rainfall by spilling water from the stilling basin. Inset is a scale image of the prismatic, polycarbonate diffuser plate used as the roughness surface in the experiments. Indentions are approximately 1 mm deep.

pumps controlled the rain intensity and the oscillation rates were computer controlled. A full cycle up and down the length of the flume was completed every 22 s.

We applied differing spatial densities of 500–590 μm silica sand particles to the upslope end of the flume surface and then washed-off the particulate with varying combinations of upslope flow and rainfall rates. Although the sand particles are at the larger-sized end of the range of material typically washed-off of urban surfaces (Sansalone et al., 1998), 500–590 μm particles were suitable to illustrate typical wash-off processes with our small-scale set-up, i.e., due to the particles rapid settling rate, wash-off rates were low enough to measure temporal differences in mass loss even with measurements only at one minute intervals. Upslope flow was systematically varied between 300 and 565 mL min^{-1} (equivalent to a rainfall rate of 0.48–0.90 cm min^{-1} applied to the 0.8 m flume length), and rainfall was varied between 0.07 and 0.13 cm min^{-1} (4.2 and 7.8 cm h^{-1}). The direct rainfall rates are comparable to intensities produced from a 2-year, 15-min storm and a 2-year, 60 min. storm in the Northeastern US (NOAA, 1977). Prior to each run, the bed of the flume was wetted and uniform flow was established. The particles were pre-wetted and uniformly spread across the 10 cm long application zone located 30 cm from the bottom of the roughness surface (Fig. 2). The limited 10 cm application zone establishes a distinct particulate ''pulse'' whose breakthrough is ultimately observed at the end of the flume. The small fraction of particles sometimes lost during particle application and establishment of the upslope flow were measured in a sample collected during the set-up process. In all experiments, once the initial particle distribution was established there was no discernable particle redistribution prior to initiating rainfall.

Flow off the end of the flume spilled into a stainless steel trough that diverted the sediment-laden water into a funnel fitted with a medium paper filter (Fisher Scientific). Each run was typically 10 min long. Filter paper was exchanged every minute, i.e., cumulative one-minute samples were collected, for the duration of the run. The samples were air dried, and the sand particles were transferred into a measuring tin and weighed. At the end of each run, the bed was rinsed and any remaining particles were collected, dried, and weighed to close the mass balance of particle loss. On average, >95% of initially applied particles were recovered. The upslope flows, rain intensities, particle recoveries, and coefficient of variation between duplicates are summarized in Table 1.

An empirical relationship between flow and velocity was developed from five velocity measurements made over a range of overland flow rates applied only as upslope inflow. Flow velocity was determined by measuring the time for the centroid of a pulse of dye (FD& C red dye No. 40), injected into the flow stream with a pipette, to travel 40 cm; the measurement was made over the middle section of the flume to avoid end-effects. Velocities measurements were made in triplicate and the coefficient of variation was $<\sim 5\%$.

Because the size of the characteristic roughness elements and particles are substantial fractions of the total depth of water on the flume, the effective settling depth, D, is smaller than the total water depth. The total depth was determined by weighing the entire flume while water flowed over the surface (Savat, 1977); depths were 1.1 and 1.4 mm for flows of 300 and 560 mL/min, respectively. Approximate D values can be determined by taking the total depth minus the particle diameters, ~0.5 mm. We also estimated D as the hydraulic flow depth, which does not include quiescent water between particles or roughness elements. Hydraulic depths, determined with continuity using the dye-determined velocity, were 0.6 and 0.7 mm for flows of 300 and 560 mL/min, respectively. Both estimates of D were similar and we used hydraulic depth in the model.

The settling depth is small so particles do not reach terminal velocity. Thus, due to the difficulty of direct measurement, the average particle settling rate over D was determined numerically assuming Stokes flow around a sphere. A drag adjustment factor was included since the Reynold's Number was greater than 1 (Soo, 1990). The calculated terminal velocity was compared to an experimental measurements (grains were hand-timed falling 40 cm in a 1 L graduated cylinder). Terminal velocities agreed within 10%. In the model, v_{set} was taken as 200 cm min^{-1}.

Table 1 Summary of upslope flow, rainfall rates, and particle recovery for each run

Run	Initial M_g (g cm^{-2})	Upslope flow (mL min^{-1})	Rainfall (cm min^{-1})	Recovery efficiency duplicate 1 (%)	Recovery efficiency duplicate 2 (%)	Coefficient of variation
1	0.01	310 [0.37]	0.13	101	104	0.089
2	0.02	305 [0.36]	0.13	97	88	0.223
3	0.03	305 [0.36]	0.12	99	95	0.031
4	0.05	305 [0.36]	0.12	98	100	0.100
5	0.07	310 [0.37]	0.13	98	98	0.060
6	0.05	300 [0.36]	0.07	95	95	0.098
7	0.05	560 [0.67]	0.07	96	97	0.096
8	0.05	565 [0.67]	0.12	96	95	0.178

All runs were carried out in duplicate.
(The bracketed upslope flow rates are in cm min^{-1} to facilitate direct comparison of rainfall and upslope flow. Volumetric flow = depth equivalent flow × 80 cm length × 10.5 cm width).

Model Implementation

We used a finite difference model to solve our system of equations. In addition to the sediment mass balance, Eqs. (1)–(4), the water balance at a point x is given by

$$q|_x = Px + q_0 \tag{5}$$

where P is the rain intensity per unit width (mL min^{-1} cm^{-1}), q is the flow rate per unit width (mL min^{-1} cm^{-1}), and q_0 (mL min^{-1} cm^{-1}) is the constant upslope inflow per unit width. The depth of flow at each point on the flume was determined by continuity and the experimentally derived relationship between q and the flow velocity. The momentum equation with the kinematic assumption was investigated but ultimately rejected because the Manning's roughness value varied substantially with q (Anderson et al., 1998).

The application of the Method of Characteristics to Eq. (1), (Myint U and Debnath, 1987) implies:

$$\frac{dx}{dt} = v \tag{6}$$

and

$$\frac{dM_s}{dt} = e - h \tag{7}$$

with the initial and boundary conditions of $t = 0$, $x \geqslant 0$, $M_s = 0$ and $t > 0$, $x = 0$, $M_s = 0$. Using discrete expressions for the equations, we solved the characteristic equations using an explicit finite difference model run with $\Delta t = 0.00025$ min, which was less than the minimum settling time. The spatial nodal spacing was determined by a discrete form of Eq. (6):

$$\Delta x = v\Delta t. \tag{8}$$

In brief, the inputs to the model comprise rainfall rate (P), initial upslope flow rate (q_0), initial particle spatial density (initial M_g), the particle settling rate (v_{set}), and the ''detachability'' factor (a). The model assumes steady state flow conditions. Computationally, for a given time, M_s is calculated for each cell, starting from the top of the plane, using discrete forms of Eqs. (7), (4) and (9) (an updated formulation of Eq. (3); see below). Cell size is determined using Eq. (9). With a discrete form of Eq. (2), M_g is updated after each successive new calculation of M_s.

Results

Experimental observations

Fig. 3 shows the observed mass loss rates for three runs differing only by initial particle spatial density, Runs 1, 3, and 5. For all runs, the observed data is the average of two duplicate trials. Runs with initial spatial densities of 0.01 and 0.03 g cm^{-2} have similarly shaped mass loss curves in which rates vary in magnitude in proportion to the initial spatial density. However, the mass loss curve of Run 5 skews to the right and has a maximum peak lower than would be expected in comparison to the lower spatial density runs. These findings suggest that above a spatial density of approximately 0.03 g cm^{-2}, interaction between particles may become significant, thus requiring adjustment of Eq. (3).

In Fig. 4, symbols indicate the experiment data points. Fig. 4 shows three runs with identical initial particle spatial densities but varying overland flow rates and precipitation rates. Overall, the most rapid breakthrough and highest peaks occur, as expected, with the highest combination of rainfall and upslope flow. Time of breakthrough, time of peak, and the magnitude of the peak decline with rainfall

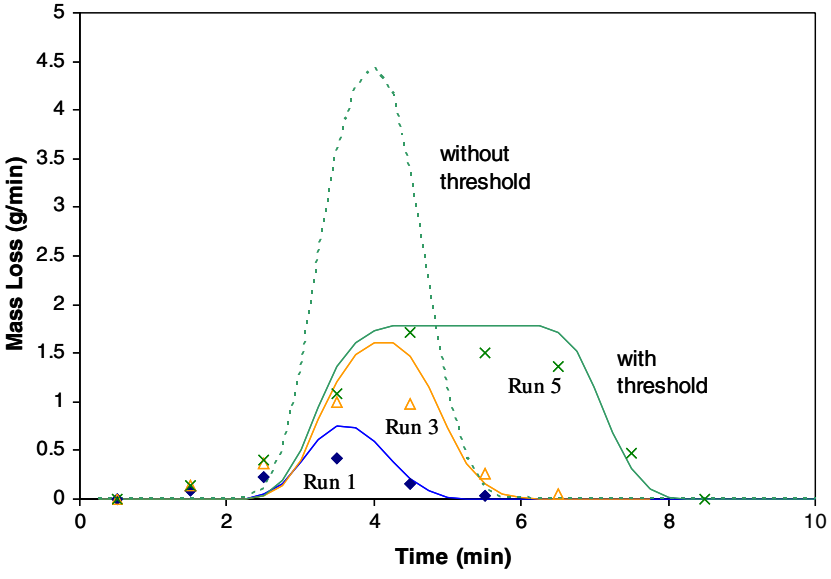

Figure 3 Model fitted to observed mass loss for experiments with varying initial spatial densities. Solid lines are model results while points are observations (circles: initial M_g 0.01 g cm^{-2}; triangles: initial M_g 0.03 g cm^{-2}; crosses: initial M_g 0.07 g cm^{-2}; diamonds: initial M_g 0.01 g cm^{-2}). As the spatial density of particles increase above a threshold of approximately 0.03 g cm^{-2}, the breakthrough curve begins to plateau. The dotted line shows model output when a maximum threshold on particle loss is not included. (See Table 1 for other relevant experimental data.)

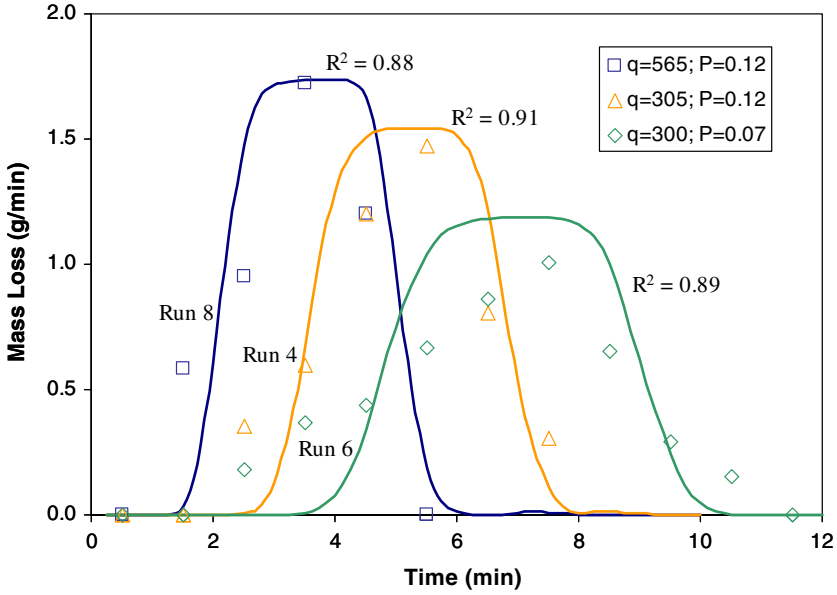

Figure 4 Model fitted to observed mass loss for experiments with varying rainfall and overland flow rates. Initial M_g is 0.05 g/cm^2 for all runs. The rainfall rate (P) (cm min^{-1}) and upslope flow rate (q) (mL min^{-1}) are indicated. Solid lines are model results while points are observations (squares: $q = 565/P = 0.12$; triangles: $q = 305/P = 0.12$; diamonds: $q = 300/P = 0.07$.)

rate and overland flow rate, although clearly not in proportion to declining upslope flow or precipitation. Also apparent is a rising leg that initially increases slowly and then rapidly rises to the peak. Visual observation during the experiments suggests that some rapid particle dispersion occurs from the front edge of the particulate pulse, possibly due to a small fraction of particles exhibiting a degree of hydrophobicity that makes them less prone to settle out.

Model Results

As suggested by the finding illustrated in Fig. 3, to account for variation in mass loss with particle spatial density, further refinement of the mass loss rate function — Eq. (3) — was undertaken. Several options for modifying Eq. (3) were considered, but the most parsimonious and most successful as based on model fitting was to establish a maximum threshold for M_g:

$$e = aPM_g \quad M_g < M_0$$
$$e = aPM_0 \quad M_g \geqslant M_0 \qquad (9)$$

where M_0 is the spatial density at which particles no longer move without measurable interaction with other particles. As an illustration, with the inclusion of this constraint, peak mass loss for Run 5 plateaued at a constant rate over several minutes, closely matching the experimental observations (Fig. 3). Based on the best fit of model results to the observed data of Runs 4 and 5 (Table 1), an average M_0 was determined to be 0.036 g cm^{-2}. The parameter a was held constant at a value of 440 cm^{-1} while determining the best fit M_0.

The model was fit to all observed runs. A single parameter was used as a calibration factor, a. The parameter a and the R^2 value for each run are presented in Table 2. The a values appear to vary with rainfall rate. For a rainfall rate of 0.12 cm min^{-1}, a is approximately 440 cm^{-1}; for a rainfall rate of 0.07 cm min^{-1} a is approximately 565 cm^{-1}.

Fig. 4 illustrates the models agreement with the duplicate-averaged results from Runs 4, 6, and 8. From this visual comparison, it is apparent that the model captures time of breakthrough, time of peak, and magnitude of peak reasonably well for a range of rainfall rates and overland flow rates. The comparison of all observed and modeled loss rates are

Table 2 Summary of model parameters and quality of fit for each model run

Run	Initial M_g (g cm^{-2})	Upslope Flow (mL min^{-1})	Rainfall (cm min^{-1})	M_0 (g cm^{-2})	a (cm min^{-1})	R^2
1	0.01	310	0.13	0.036	430	0.90
2	0.02	305	0.13	0.036	420	0.75
3	0.03	305	0.12	0.036	470	0.96
4	0.05	305	0.12	0.035	440	0.91
5	0.07	310	0.13	0.037	440	0.97
6	0.05	300	0.07	0.036	560	0.89
7	0.05	560	0.07	0.036	570	0.82
8	0.05	565	0.12	0.036	420	0.88

The model was fit to the average observed values for each run. Given the standard sand grain size and roughness surface, the parameter a appears to vary only with rainfall rate.

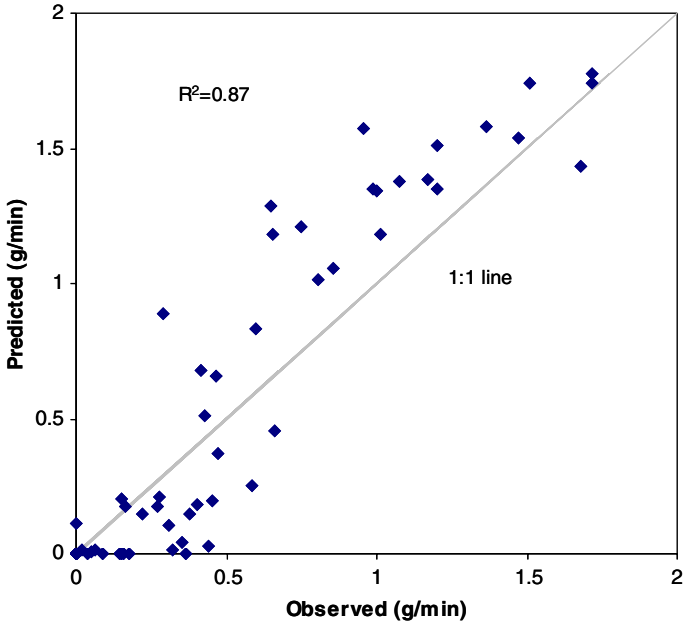

Figure 5 Comparison of observed versus predicted mass loss values for all runs. Observed values are average of duplicates for each run. Modeled values are the cumulative mass loss over a minute interval — the quantity directly measured in the experiment.

shown in Fig. 5. Note, in Fig. 5 modeled data points were computed as the cumulative mass loss over each minute sampling increment, the actual quantity directly measured in the experiment; other figures show the continuous mass loss rate. Fig. 5 indicates that the model slightly underpredicts at low values and overpredicts and higher values. This systematic error is due to the fact that the model does not include a mechanism to account for the early breakthrough of a small fraction of the total particles (i.e. slightly hydrophobic particles that do not readily settle). Low concentration values resulting from this limited early breakthrough are not well replicated by the model. Thus, based on conservation of mass, mass loss predictions when the bulk of the particles breakthrough are slightly too high.

Discussion

The proposed model establishes distinct roles for rainfall and overland flow in inducing wash-off when overland flow is below a critical shear stress: rainfall dislodges particles while overland flow transports the particles. Unlike previous wash-off models (Akan, 1988; Deletic et al., 1997), the model incorporates a function for particle settling. In the other model formulations, once a particle was entrained, it would leave the system, similar to the anticipated behavior of a dissolved substance. In reality, the flow and the rain interact in more complicated ways to control rain-flow transport. The flow controls how far an ejected particle moves with deeper flows and/or faster flows increasing particle ''jump'' distances by increasing settling time and lateral saltation, respectively. Thus, models that do not account for particle settling do not capture the fundamental rain-induced transport processes.

Additionally, the model recognizes interaction between particles by including a maximum ejection rate for a given rainfall rate. Given that the rate of mass loss cannot increase if $M_g > M_0$ suggests that surface particles shield underlying particles from the effect of rain drops. Thus, once the particle spatial density exceeds M_0, the system acts similarly to a deep soil with minimal particle adhesion.

Determining *a* from fundamentals

For implementation of the model to realistic situations, it is useful to derive the parameter a on physical grounds. Lisle et al. (1998) conceptualized particle movement as a two-state Markov process, i.e., the particle is either in a state of motion or a state of rest and is unaffected by its previous history of movement. Lisle et al. (1998) proposed a physical meaning for the probability of being in motion per unit time and arrived at an expression analogous to a in Eq. (9):

$$a \approx \frac{A_0}{V} \tag{10}$$

where A_0 (cm^2) is the impact area of a single rain drop and V (cm^3) is the drop volume.

The average a value in our study is $\sim$440 cm^{-1}, implying an A_0 radius approximately seven times the average drop radius of 0.08 cm at a rainfall rate of 0.12 cm min^{-1}. Previous studies have measured the radius of the subsurface cavity generated by a drop falling into a shallow liquid, which seems like a reasonable means to estimate A_0. For a 0.08 cm radius drop falling near terminal velocity (similar to our experiments), cavity radii were found to be between four (Macklin and Metaxas, 1976) and seven (Prosperitti and Oguz, 1993) times the drop radius.

An increase in a value with decreasing rainfall rate may be partially due to an increase in average drop size. As noted previously, the drop size slightly increases with decreasing P. While an increase in drop radius would be expected to decrease a given no change in ratio between drop size and cavity size, Macklin and Metaxas'data (1976)

suggest the ratio is not constant. The a parameter actually increases since the ratio between drop size and cavity size increases faster than the ratio between drop cross-sectional area and volume decreases. However, while Macklin and Metaxas' (1976) data suggest the correct trend, the magnitude of the trend does not entirely explain the difference of more than 100 cm^{-1} between a values at the two rainfall rates. Further experimentation is needed to see if the difference in a is partially due to experimental variability or actual physical factors.

Fraction of total wash-off due to rain-transport

It is unclear how rain-flow transport and shear-induced transport interact when both processes are present, although, literature suggests that overland shear stress supercedes rain-flow transport as flow depths and/or slopes become large (Moss et al., 1979). However, even in large intensity events, due to flow accumulation, one would expect overland-shear to become important only on the downslope end of longer reaches. Thus, even considering the accepted dogma, rain-flow transport would always play a role in some parts of the landscape. By way of example, we used 2-year 15 min and 2-year 60-min rainfall intensity data for the Northeastern United States (NOAA, 1977) to determine the accumulated flow length at which overland shear forces exceed the thresholds given by the Shield's diagram. Flow depths were estimated using Manning's Equation with slope = 0.02 and n = 0.03 (Anderson et al., 1998). For the 15 and 60-min storms, the reach length would need to exceed approximately 2 m and 3.5 m, respectively, for 100 μm particles to even start to be moved be by shear (5 and 9 m for 545 μm particles). In a typical urban environment consisting of roadways, sidewalks, and roof surfaces, one would expect that the typical continuous reach length would be on the order of 10 m, leaving a sizable fraction of surfaces unaffected by overland shear forces, and suggesting observed wash off in these areas is due to rain-flow transport.

We also ran some simple supplementary experiments with our experimental set-up to investigate the role of roughness on the critical shear stress. While the Shield's curve has been used to estimate the critical shear stress on impervious surfaces, it was originally developed from data in channels with loose beds. We applied upslope flow (with no rain) at rates for which the shear should have exceeded Shield's critical shear; Specifically, we used a 1600 mL min^{-1} flow and observed minimal particle loss even though the Shield's curve predicts a critical shear threshold near 1100 mL min^{-1} flow. We suspect that surface roughness may increase the critical shear stress, thus further increasing the fraction of the urban landscape not necessarily subject to wash-off from overland shear forces.

Characterizing surface roughness

The experimental results in this work are likely dependent on the characteristics of the roughness surface. While a highly regular rough surface was used to minimize confounding experimental factors, the surface is not necessarily a perfect proxy for the more irregular rough surfaces actually found in the environment, such as asphalt and concrete. From experimentation with other surfaces, it is apparent that in addition to simply using the characteristic roughness length to describe surfaces, another critical parameter is the fraction of the surface covered by ''deep'' depressions (deep relative to the particle size and drop energy). The polycarbonate diffuser plate used as a surface in this experiment consisted of a regular pattern of adjacent, but shallow depressions. All particles were regularly trapped, but no particles were retained for an extended time. However, other surfaces briefly tested in this work — such as 2 mm glass beads partially submerged in resin — included deep depressions and led to particle retention and the observation of a lengthy tail in the breakthrough curve (Fig. 6). Impervious surfaces found in the built environment are likely to include a range of recess depths resulting in a range of retention times and complex breakthrough curves. Modeling realistic built surfaces will most likely require a more rigorous method to quantify the characteristics of the surface and is, indeed, the focus of follow-up research to this study.

Conclusions

The primary objective of this work was to quantify the roles of overland flow and rainfall in particulate wash-off and

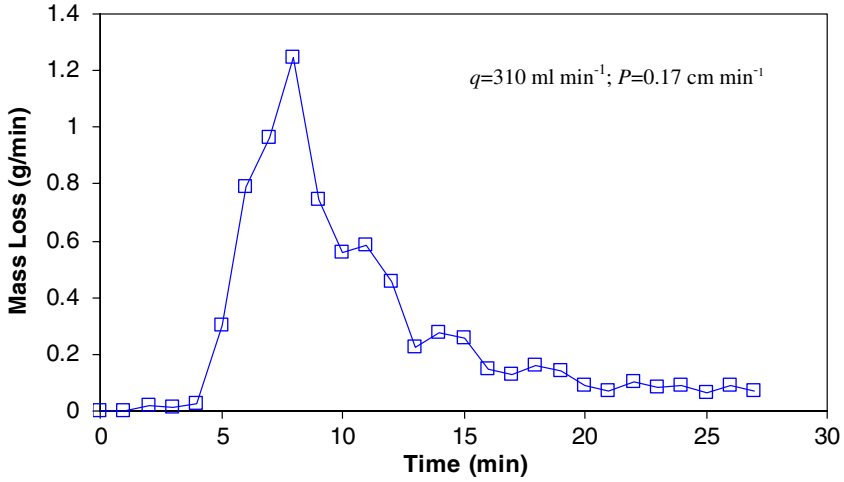

Figure 6 Mass loss curve for surface with deep depressions. The long tail is due to particle detention in the depressions.

transport on rough, impervious surfaces when overland shear forces are below a critical threshold for inducing particle movement.

Based on experimental observations, we proposed a model that conceives of particulate ejection and transport on impervious surfaces of moderate slope as a saltation-type process induced by rainfall. This process is similar to so-called 'rain-flow transportation' first noted by Moss et al. (1979) in looking at erosion of soil beds and modeled for soils by Hairsine and Rose (1991).

Overall, the model begins to connect wash-off theory into the much more extensive body of research on soil erosion. However, two features distinguish wash-off from soil erosion: the process quickly becomes sediment limited and the roughness features do not simply affect hydraulic flow characteristics but also the availability of particles. Additional investigation is needed into these two realms to more fully develop the physical wash-off mechanisms.

References

Akan, A.O., 1988. Pollutant washoff by overland flow. Journal of Environmental Engineering 113 (4), 811–823.

Anderson, D.A., Huebner, R.S., Reed, J.R., Warner, J.C., Henry, J.J., 1998. Report prepared for National Cooperative Highway Research Program. Improved Surface Drainage of Pavement. NHCRP Web Document 16. National Academy of Sciences.

Bicknell, B.R., Imhoff, J.C., Kittle, J.L., Jr., Donigian, A.S., Jr., Johanson, R.C., 1997. Hydrological simulation program – Fortran, User's manual for version 11: U.S. Environmental Protection Agency, National Exposure Research Laboratory, Athens, Ga., EPA/600/R-97/080, 755 p.

Deletic, A., Maksimovic, C., Ivetic, M., 1997. Modelling of storm wash-off of suspended solids from impervious surfaces. Journal of Hydraulic Research 35 (1), 99–117.

Foster, G.R., Meyer, L.D., 1975. Mathematical simulation of upland erosion by fundamental erosion mechanics. In: Present and Perspective Technology for Predicting Sediment Yields and Sources – Proceedings of the Sediment-Yield Workshop, Dept, S.U., of Agriculture Sedimentation laboratory, Oxford, MI, November 1972 (ARS-40) USDA, Washington DC, pp. 190–206.

Gao, B., Walter, M.T., Steenhuis, T.S., Parlange, J.-Y., Nakano, K., Hogarth, W.L., Rose, C.W., 2003. Investigating ponding depth and soil detachability for a mechanistic erosion model using a simple experiment. Journal of Hydrology 277 (1–2), 116–124.

Gao, B., Walter, M.T., Steenhuis, T.S., Hogarth, W.L., Parlange, J.-Y., 2004. Rainfall induced chemical transport from soil to runoff: Theory and experiments. Journal of Hydrology 295 (1–4), 291–304.

Gao, B., Walter, M.T., Steenhuis, T.S., Parlange, J.-Y., Richards, B.K., Hogarth, W.L., Rose, C.W., 2005. Investigating raindrop effects on transport of sediment and non-sorbed chemicals from soil to surface runoff. Journal of Hydrology 308, 313–320.

Graf, W.H., 1971. Hydraulics of Sediment Transport. McGraw-Hill, New York.

Hairsine, P.B., Rose, C.W., 1991. Rainfall detachment and deposition: sediment transport in the absence of flow-driven processes. Soil Science Society of America Journal 55, 320–324.

Jayawardena, A.W., Bhuiyan, R.R., 1999. Evaluation of an interrill soil erosion model using laboratory catchment data. Hydrological Process 13, 89–100.

Kirkby, J.M., 1980. The Problem. In: Kirkby, M.J., Morgan, R.P.C. (Eds.), Soil Erosion. John Wiley and Sons Ltd, New, pp. 1–16.

Laflen, J.M., Elliot, W.J., Simanton, J.R., Holzhey, C.S., Khol, K.D., 1991. WEPP soil erodibility experiments for rangeland and cropland soils. Journal of Soil Water Conservation 49 (1), 39–44.

Laws, J., Parsons, D., 1943. The relation of raindrop size to intensity. Eos Transactions. AGU 24, 452–460.

Liebenow, A.M., Elliot, W.J., Laflen, J.M., Kohl, K.D., 1990. Interrill erodibility – collection and analysis of data from cropland soils. ASAE Transactions 33 (6), 1882–1888.

Lisle, I.G., Rose, C.W., Hogarth, W.L., Hairsine, P.B., Sanders, G.C., Parlange, J.-Y., 1998. Stochastic sediment transport in soil erosion. Journal of Hydrology 204, 217–230.

Macklin, W.C., Metaxas, J.G., 1976. Splashing of drops on liquid layers. Journal of Applied Physics 47 (9), 3963–3970.

Moss, A.J., Walker, P.H., Hutka, J., 1979. Raindrop-stimulated transportation in shallow water flows: an experimental study. Sedimentary Geology 22, 165–184.

Myint U, Tyn, Debnath, L., 1987. Partial Differential Equations for Scientists and Engineers, third ed. Elsevier, New York.

NOAA, 1977. Five to 60-minute precipitation frequency for the eastern and central US. NOAA Technical Memorandum NWS HYDRO-35, Silver Spring, Md.

Prosperitti, A., Oguz, H.N., 1993. The Impact of drops on liquid surfaces and the underwater noise of rain. Annual Reviews of Fluid Mechanics 25, 577.

Rose, C.W., 1985. Developments in soil erosion and deposition models. Advances in Soil Science 2, 1–63.

Rose, C.W., Hogarth, W.L., Sander, G., Lisle, I., Hairsine, P., Parlange, J.-Y., 1994. Modeling processes of soil erosion by water. Trends in Hydrology 1, 443–451.

Sansalone, J.J., Koran, J.M., Smithson, J.A., Buchberger, S.G., 1998. Physical characteristics of urban roadway solids transported during rain events. Journal of Environmental Engineering. 124 (5), 427–440.

Sartor, J.D., Boyd, G.B., 1972. Water Pollution Aspects of Street Surface Contaminants. EPA-R2-72-081. US EPA, Washington, D.C.

Sartor, J., Boyd, G.B., Agardy, F.J., 1974. Water pollution aspects of street surface contaminants. Journal of the Water Pollution Control Federation 46 (3), 458–465.

Savat, Jan., 1977. The hydraulics of sheet flow on a smooth surface and the effect of simulated rainfall. Earth Surface Processes 2, 125–140.

Sharma, P.P., Gupta, S.C., Foster, G.R., 1993. Predicting soil detachment by raindrops. Soil Science Society of America Journal 57, 674–680.

Sharma, P.P., Gupta, S.C., Foster, G.R., 1995. Raindrop-induced soil detachment and sediment transport from interrill areas. Soil Science Society of America Journal 59, 727–734.

Soo, S., 1990. Multiphase Fluid Dynamics. Glower Technical, Alershot-Brookfield.

Tsihrintzis, V.A., Hamid, R., 1998. Runoff quality prediction from small urban catchments using SWMM. Hydrological Processes 12, 311–329.

Vaze, C., Chiew, F.H.S., 2003. Study of pollutant washoff from small impervious experimental plots. Water Resources Research, V 39 (6), HWC 3-1–HWC 3-9.